CONF-970231--6
SAN097-0347C
SAND--97-0347C

Quantum Cascade Light Emitting Diodes Based on Type-II Quantum Wells

Chih-Hsiang Lin, Rui Q. Yang, D. Zhang, S. J. Murry and S. S. Pei
Space Vacuum Epitaxy Center, University of Houston, TX 77204-5507

A. A. Allerman and S. R. Kurtz
Sandia National Laboratories, Albuquerque, NM 87123-0603

ABSTRACT

We have demonstrated room-temperature CW operation of type-II quantum cascade (QC) light emitting diodes at 4.2 μm using InAs/InGaSb/InAlSb type-II quantum wells. The type-II QC configuration utilizes sequential multiple photon emissions in a staircase of coupled type-II quantum wells. The device was grown by molecular beam epitaxy on a p-type GaSb substrate and was composed of 20 periods of active regions separated by digitally graded quantum well injection regions. The maximum average output power is about 250 μW at 80 K, and 140 μW at 300 K at a repetition rate of 1 kHz with a duty cycle of 50%.

Keywords: MBE, Mid-IR, Infrared, quantum well, type-II quantum well, quantum cascade, laser

1. INTRODUCTION

Mid-infrared (MIR) lasers emitting from 3 to 5 μm have important applications in infrared (IR) countermeasures, IR lidar, remote sensing, and environmental monitoring such as detection of trace gases, hydrocarbon fuel emission, and other common pollutants. However, both military and commercial MIR systems are limited due to a lack of adequate sources. Currently, MIR solid state lasers tend to be bulky with little wavelength agility, while optical parametric oscillators (which use a nonlinear crytal to down convert or up convert the output wavelength of pump sources) are complex and expensive. Semiconductor diodes lasers have significant advantages in terms of cost, volume, weight, relaibility, power dissipation, and manufacture. The availability of compact high-power MIR semiconductor diode lasers operating at ambient or thermo-electrically cooled temperatures would significantly enhance the capability of current MIR technology.

IV/VI Lead-salt lasers emitting at wavelengths longer than 3 μm have been available for a number of years. These lasers with emission wavelengths of 4 μm have exhibited pulsed operation at temperatures up to 290 K [1], and cw operation up to 223 K [2]. However, they are not expected to produce high

output power (>1 mW) because of the low thermal conductivity of lead-salt alloys, and their susceptibility to damage. For narrow bandgap II/VI semiconductors such as HgCdTe alloys, the first reported laser diodes operated under pulse injection up to 90 K at the wavelength of 2.86 μm. It is thus very desirable to develop semiconductor lasers using III-V alloys, because these materials offer good metallurgical and thermal properties and because better-quality substrates are readily available.

Recently, MIR lasers utilizing Sb-based type-I structures are showing a stead progress [3-9]. Room-temperature operation of laser diodes at wavelengths shorter than 2.8 μm has been realized [3-5]. However, due to the intrinsic nature of type-I interband transitions, the lasing wavelength is limited to the material bandgap, and the device performance suffers from non-radiative Auger recombination. For wavelength longer than 4 μm, MIR lasers based on type-I interband structure has proven to be quite challeging.

MIR lasers based on InAs/InGaSb type-II superlattices (SLs) [10] have achieved similar performance as those based on Sb-based type-I structures. A maximum operating temperature T_{max} = 255 K was achieved at 3.2 μm [10]. By simply changing the InAs and InGaSb layer thicknesses, the lasing wavelength of type-II InAs/InGaSb lasers could vary from MIR to long IR. This is an important advantage of InAs/InGaSb type-II lasers compared to the Sb-based type-I devices in terms of epitaxy growth, since the composition control, composition uniformity, and growth reproducibility of InGaAsSb, InAlAsSb, and AlGaAsSb are very difficult. Additionally, due to the unique feature of type-II structures, the Auger recombination could be deamatically suppressed through careful bandgap engineering. For the gain spectrum, InAs/InGaSb type-II structures can display strong oscillator strength as long as the the layers are thin enough to allow enough interpenetration of the electron and hole wavefunctions, and hence large gain should be attainable from type-II structures. Recently, we have demonstrated above room-temperature operations of optically-pumped MIR lasers based on InAs/InGaSb/AlSb type-II quantum wells (QWs) with record maximum operating temperature T_{max} and characteristic temperature T_o [11-15]. Laser emission at 4.2 to 4.5 μm has been observed at temperatures up to 310 K, and a peak output power exceeding 2 W/facet was observed at 200 K [15].

Type-I quantum cascade (QC) lasers [16] which utilize sequential multiple photon emissions between subbands in a staircase of coupled type-I InGaAs/InAlAs QW structure promises significantly improved performance of MIR lasers. The recent demonstrations of a high power room-temperature QC laser at 5 μm [16] and a long wavelength IR (~11 μm) QC laser operating up to 200 K [17] indicate a great potential for the QC configuration. The QC lasers are especially suitable for obtaining high output powers. However, the type-I QC lasers still have a relatively low radiative efficiency ($<1x10^{-3}$) due to a fast non-radiative phonon relaxation between subbands, which leads to a high threshold current density and substantial heating.

In contrary, the type-II QC lasers, as originally proposed in Ref. 18, are based on interband transitions where the phonon relaxation is intrinsically suppressed due to the opposite curvatures of conduction and valence band structures. Figure 1 shows the schematic drawing of a n-type QC laser based on type-II QWs [19, 20]. Under a forward bias, electrons are injected from an injection region into the InAs well. The InGaSb, AlSb, and GaSb layers are thick enough to efficiently block the direct runneling of electrons out of the InAs well, resulting in a reduced leakage current.

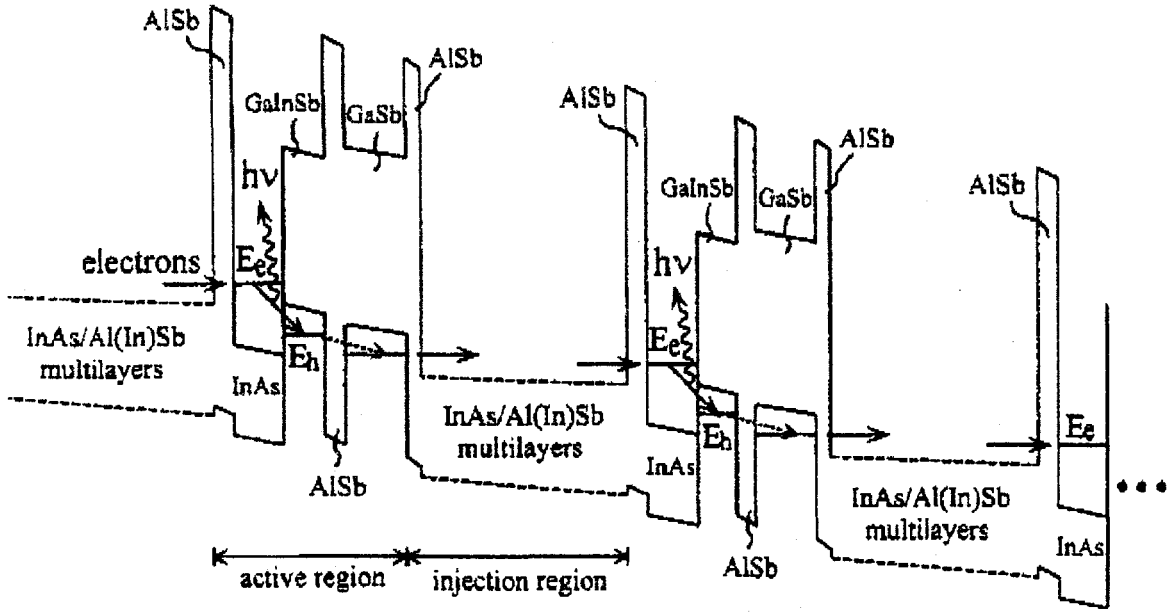

Figure 1. Schematic drawing of a n-type-QC structure based on type-II QWs.

2. EXPERIMENT

The type-II QC light emitting diode (LED) was composed of 20 periods of active regions separated by *n*-type injection regions which serve both as the collectors for the preceding active regions and emitters for the following ones. As shown in Figure 1, the active region was composed of several couples QWs, which were sequentially made of 23 Å AlSb, 25.5 Å InAs, 34 Å InGaSb, and 15 Å AlSb layers. The injection region consists of digitally graded InAs/AlSb (InAlSb) QWs in which the InAs layers are Si doped at 6×10^{17} cm^{-3}, and the AlSb and InAlSb layers are undoped. The whole device structure is strain balanced and lattice matched to the GaSb substrate. To improve the power efficiency, we have been careful in the design of active regions and injection regions in order to minimize the losses due to interband and intersubband absorption, and Auger recombination. Under a forward bias, electrons are injected from an injection region into the level E_e which is in the bandgap region of the adjacent InGaSb layer. Since the electrons are effectively confined in the InAs well with the InGaSb, AlSb, and GaSb barrier layers, they tend to relax to the hole state E_h in the adjacent valence band QW. The resulting photon emissions are shown in Figure 1. Therefore, the leakage current is reduced. Electrons at state E_h will then cross the thin AlSb barrier and GaSb layer by tunneling and scattering into the conduction band of the next injection region because of a strong spatial interband coupling (an unique feature existed in Sb-based type-II heterostructure), and are ready for the next interband transition. Since the relaxation time from E_e to E_h is much longer than the carrier transportation time at E_h, a population inversion is easily established.

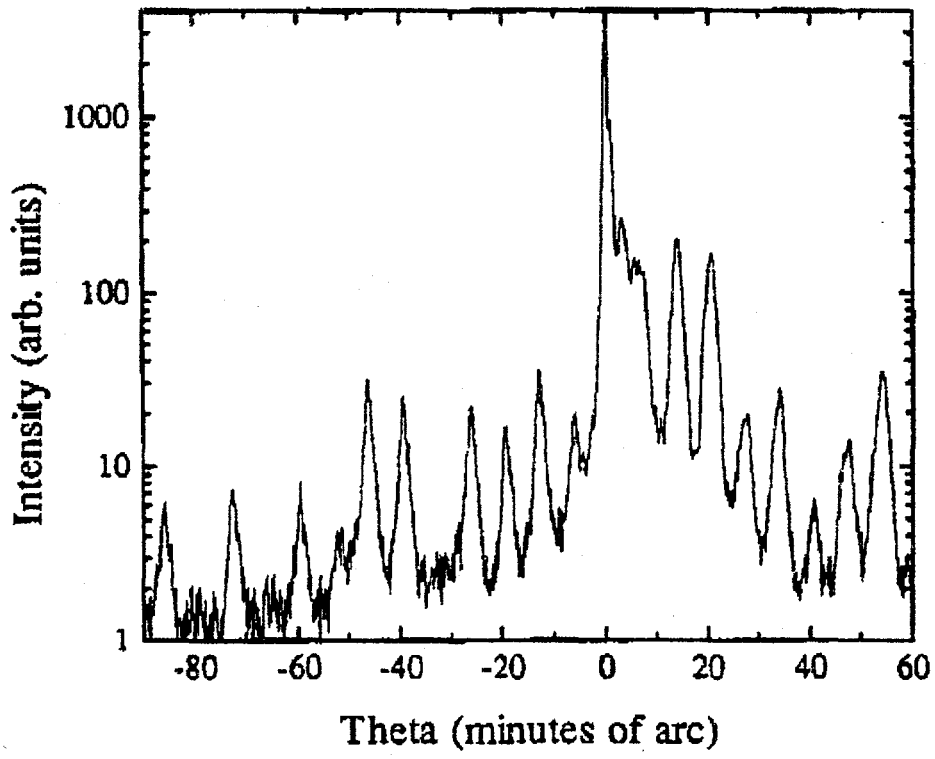

Figure 2. 004 DCXRD spectrum of a type-II QC device.

The type-II QC LEDs were grown in a Riber 32 molecular beam epitaxy (MBE) system on a p-type GaSb substrate using an EPI As valved cracker cell and an EPI Sb cracker cell. A 3000-Å GaSb buffer layer adjacent to the substrate was grown at 510 °C. The InAs/AlSb cladding layers and the active region was grown at 440 °C. During the growth, the GaSb layers displayed good 1× 3 reflection high-energy electron diffraction (RHEED) pattern and the InAs layers exhibited good 2×1 RHEED patterns. After growth, the sample was annealed at 490 C for 10 minutes. Growth rates were calibrated to within ±2 % using RHEED and were confirmed by double-crystal x-ray diffraction (DCXRD) measurements. The background doping density was low 10^{15} cm^{-3} n-type for InAs and was about 2×10^{16} cm^{-3} p-type for GaSb. Using the same growth rate for InAs and GaSb, the background Sb in InAs layers was less than 1% and the background As in GaSb was less than 3%, with a V/III BEP ratio of 3 for InAs and 2 for GaSb. The BEP ON/OFF ratio with shutters opened or closed was about 8 for As_2, and was about 160 for Sb_1. When the Sb/Ga V/III BEP ratio was increased, the background As in GaSb decreased. However, the background Sb in InAs layers was not sensitive to the As flux. This implies that the sticking coefficient of background Sb in InAs at 440 °C is almost 100%. From photoluminescence (PL) spectra, the material quality of GaSb/AlSb QWs is not sensitive to the Sb/Ga V/III BEP ratio as long as the ratio is larger than 1.8. In order to improve the layer thickness and composition control, we have also investigated the flux transients of In, Ga, and Al effusion cells due to shutter operations [21]. Using the EPI SUMO cells for In

and Ga, the short term flux transient has been reduced from 15% to 6%. Figure 2 shows the DCXRD spectrum of a type-II QC LED. The figure shows the substrate peak surrounded by several orders of well defined SL peaks, which are indicative of sharp interface quality and good composition control.

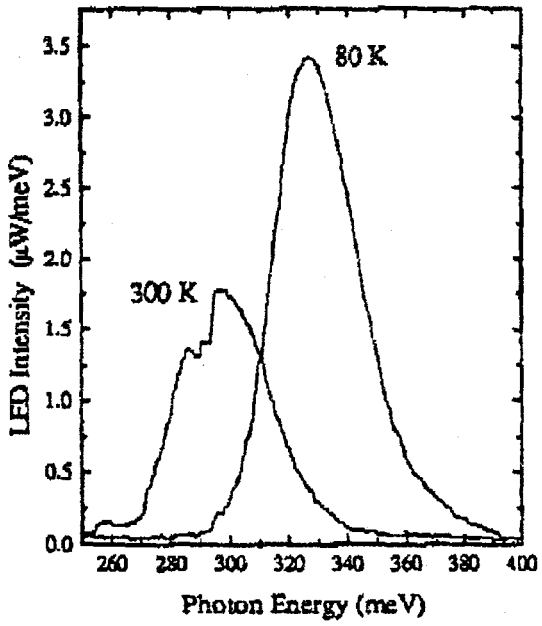

Fig. 3a. EL spectra at 80 K and 300 K.

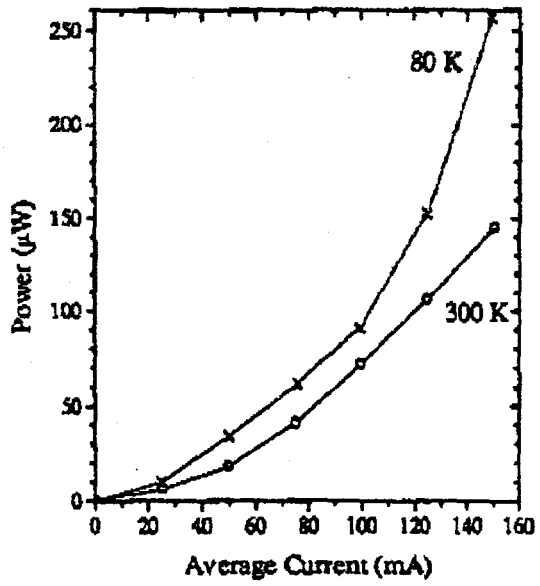

Figure 3b. Average output power vs. average current.

After characterized by DCXRD measurement, Ti/Au ohmic contacts were provided to the n-type InAs contact layer and the p-type GaSb substrate. However, after processing, we have noticed some striations across the devices. This is possibly due to the poor crystal quality of the GaSb substrate, since there have been several perpendicular striation lines appeared on the surface right after MBE growth, and the DCXRD spectrum of this device showed clear satellite peaks. It is known that if the crystal defect density is large, this phenomenon will happen after several thermal cycles even without any epitaxy growth. Further investigations will be performed to solve this problem. Current pulse was then injected into the devices at a repetition rate of 1 KHz with a duty cycle of 50%. The light was emitted from the top and collected into a 2mm×2mm InSb photodetector for relative power measurements. For absolute power measurements, the device was mounted inside a parabolic collector, and an 1 cm-diameter pyroelectric power meter was placed at the face of the collector. As shown in Figure 3a, the electroluminescence (EL) spectrum at 80 K shows a peak at 327 meV (3.8 μm) with a full width at half maximum (FWHM) of 32 meV, and at 300 K the peak is red shifted to 296 meV (4.19 μm) with a FWHM of 36 meV due to the smaller bandgap at higher temperatures. The peak wavelengths agree well with our calculations using the $k \cdot p$ envelope wavefunction method including the strain effect. Figure 3b shows the average output power vs. average injection current at 80 K and 300 K. With an average current of 150 mA, the maximum average output power was about 250 μW at 80 K, and was 140 μW at 300 K, which were much larger

than the available output power (~10 μW) of commercial LEDs. Compared to our first reported type-II QC LED [22], we have improved the output power by more than three orders of magnitude. This significant improvement is mainly attributed to the improved design of the active region and injection region in attempts of minimizing the losses due to the interband and intersubband absorption, and Auger recombination, enhancing the wavefunction overlap between E_e and E_h states, and better match to the substrate. From 80 K to 300 K, the output power was only reduced by a factor less than two. We have noticed this weak temperature dependence of output power from all of our type-II QC LEDs [22, 23]. However, due to the small injection current density, we can not conclude that Auger recombination has been dramatically suppressed in these type-II QC devices, as have been predicted. However, the preliminary results are very promising. Figure 3c shows the I-V curves of the device at 80 K and 300 K. From 80 K to 300 K, the resistance was reduced from 105 Ω to 36 Ω due to the carrier thermal excitation. Most of the resistance at low forward bias was contributed by the injection region, since the energy levels in the digitally graded QWs would not be aligned until the required electric field was applied. With larger forward biases, the resistance will decrease.

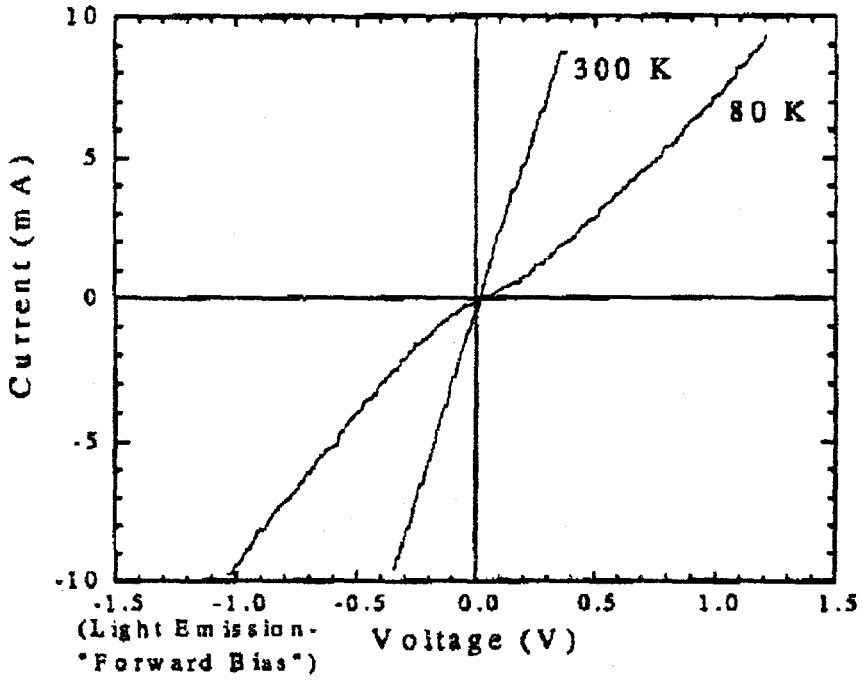

Fig. 3c. Current vs. applied voltage of the type-II QC LED at 80 K and 300 K.

3. CONCLUSIONS

We have reported the room-temperature cw electroluminescence of type-II QC device at 4.2 μm. With an average current of 150 mA, the maximum average output power was about 250 μW at 80 K, and 140 μW at 300 K, which were much larger than the available output power (~10 μW) of commercial LEDs.

With improved design of the active region and injection region, we have improved the output power more than three orders of magnitude compared to our first reported type-II QC LED. However, the performance of this device is still strongly limited by the poor material quality (striations on the surface), possibly due to the poor crystal quality of the GaSb substrate. Further improvements in the substrate quality and MBE growth will significantly improve the device performance. To achieve room-temperature MIR lasers based on type-II QC configuration, further investigations in the device design, especially the carrier transportation and Auger recombination, will be the key issues.

4. ACKNOWLEDGMENTS

The authors at UH thank J. R. Meyer and H. Q. Le for helpful discussion, H. C. Liu for the detailed characterizations of earlier devices, and C.-H. Thang for DCXRD measurement. The work at UH is partially supported by NASA contract No. NAGW-977 and TcSCH. The work at Sandia National Laboratories is supported by Dept. of Energy under Contract No. DE-AC04-94AL8500.

REFERENCES

1. Z. Shi, M. Tacke, A. Lambrecht, and H. Bottner, Appl. Phys. Lett. 66, 2537 (1995)
2. Z. Feit, M. McDonald, R. J. Woods, V. Archambault, and P. Mak, Appl. Phys. Lett. 68, 738 (1996).
3. H. Lee, P. K. York, R. J. Menna, R. U. Martinelli, D. Z. Garbuzov, S. Y. Narayan, and J. C. Connolly, Appl. Phys. Lett. 66, 1942 (1995).
4. D. Z. Garbuzov, R. U. Martinelli, R. J. Menna, P. K. York, H. Lee, S. Y. Narayan, and J. C. Connolly, Appl. Phys. Lett. 67, 1346 (1995).
5. H. K. Choi and S. J. Eglash, Appl. Phys. Lett. 61, 1154 (1992).
6. H. K. Choi, G. W. Turner, M. J. Manfra, and M. K. Connors, Appl. Phys. Lett. 68, 2936 (1996).
7. H. K. Choi, G. W. Turner, and M. J. Manfra, Electron. Lett. 32, 1296 (1996).
8. S. R. Kurtz, R. M. Biefeld, L. R. Dawson, K. C. Baucom, and A. J. Howard. Appl. Phys. Lett. 64, 812 (1994).
9. A. A. Allerman, R. M. Biefeld, and S. R. Kurtz, Appl. Phys. Lett. 69, 465 (1996).
10. R. H. Miles, D. H. Chow, Y. H. Yang, P. D. Brewer, and R. G. Wilson, Appl. Phys. Lett. 65, 1921 (1995).
11. J. I. Malin, J. R. Meyer, C. L. Felix, J. R. Lindle, L. Goldberg, C. A. Hoffman, and F. J. Bartoli, C. H. Lin, P. C. Chang, S. J. Murry, R. Q. Yang, and S. S. Pei, Appl. Phys. Lett. 68, 2976 (1996).
12. J. I. Malin, C. L. Felix, J. R. Meyer, C. A. Hoffman, and J. F. Pinto, C. H. Lin, P. C. Chang, S. J. Murry, and S. S. Pei, Electron. Lett. 32, 1593 (1996).
13. C. H. Lin, S. J. Murry, D. Zhang, P. C. Chang, Y. Zhou, and S. S. Pei, J. I. Malin, C. L. Felix, J. R. Meyer, C. A. Hoffman, and J. F. Pinto, J. Crystal Growth, in press.
14. C. H. Lin, P. C. Chang, S. J. Murry, D. Zhang, R. Q. Yang, and S. S. Pei, J. I. Malin, J. R. Meyer, C. L. Felix, J. R. Lindle, L. Goldberg, and C. A. Hoffman, J. Electron. Materials, in press.
15. C. L. Felix, J. R. Meyer, and I. Vurgaftman, C.-H. Lin, S. J. Murry, D. Zhang, and S. S. Pei, submitted to IEEE Photon. Technolo. Lett.
16. J. Faist, F. Capasso, C. Sirtori, D. L. Sivco, J. N. Baillargeon. A. L. Hutchinson, S. N. G. Chu, and A. Y. Cho, Appl. Phys. Lett. 68, 3680 (1996).

17. C. Sirtori, J. Faist, F. Capasso, D. L. Sivco, A. L. Hutchinson, and A. Y. Cho, Appl. Phys. Lett. 69, 2810 (1996).
18. R. Q. Yang, Superlattices and Microstructures, 17, 77 (1995).
19. J. R. Meyer, I. Vurgaftman, R. Q. Yang, and L. R. Ram-Mohan, Electron. Lett. 32, 45 (1996).
20. R. Q. Yang and S. S. Pei, J. Appl. Phys., 79, 8197 (1996).
21. S. J. Murry, C. H. Thang, D. Zhang, C.-H. Lin, and S. S. Pei, G. A. Patterson, submitted to J. Vacuum Science and Technol.
22. R. Q. Yang, C.-H. Lin, P. C. Chang, S. J. Murry, D. Zhang, and S. S. Pei, S. R. Kurtz, S.-N. G. Chu, and F. Ren, Electron. Lett., 32, 1621 (1996).
23. R. Q. Yang, C.-H. Lin, S. J. Murry, and S. S. Pei, H. C. Liu, M. Buchanan, and E. Dupont, submitted to Appl. Phys. Lett.

DISCLAIMER